COLLEGE OF ENGINEERING

VIRGINIA POLYTECHNIC INSTITUTE AND STATE UNIVERSITY

BLACKSBURG, VIRGINIA

VPI-Aero-026
Nov. 30, 1974

Final Report
"ANALYTICAL STUDY OF SUBSONIC TURBULENT
BOUNDARY LAYER SEPARATION INCLUDING
VISCOUS-INVISCID INTERACTION"

NASA Grant NGR 47-004-119
covering time period June, 1973 to Nov. 30, 1974

G. R. Inger
Dept. of Aerospace and Ocean Engineering
Virginia Polytechnic Institute and State University
Blacksburg, Va. 24061

l

1. INTRODUCTION

The prediction of boundary layer separation continues to be an important basic research problem in fluid dynamics with many applications in aerodynamics, propulsion, fluidics devices, etc. The numerous theoretical and experimental studies that have been carried out to date have established three important features of this problem that cannot be accounted for in the classical boundary layer theory approach. (1) Viscous-inviscid interaction: the streamwise pressure gradient is not prescribed but is an unknown determined by the boundary layer displacement thickness distribution solution. (2) Upstream influence: the local behavior at some station x is affected by conditions downstream as well as those upstream, the mathematical character of the flow being of an elliptic nature rather than parabolic (this is true even for a supersonic inviscid flow). (3) Regions of reversed flow and possible reattachment: these introduce the well-known possibility of a singularity where the wall shear vanishes plus the numerical difficulties associated with imbedded regions of reversed flow near the surface. To complement the various numerical methods that are currently being developed to treat these features (Ref. 1,2) the present paper describes an approximate analytical approach to the boundary layer separation problem for subsonic laminar separation bubble-type flows.[3]

Our analysis is based on a triple-deck flow model which is an extension of the earlier methods of Von Karman and Millikan,[4] Stratford,[5] and Curle[6] to include the aforementioned effects of viscous-inviscid interaction, upstream influence, and flow reversal and reattachment. The boundary layer is split up into two appropriately-matched regions: a thin viscous sublayer region of negligible inertia near the wall underneath a thick outer layer of nearly

1. INTRODUCTION

The prediction of boundary layer deceleration and separation in regions of adverse pressure gradient continues to be an unsolved problem of fundamental practical importance in aerodynamics. Separation, for example, not only significantly influences the local flow field but also can influence the overall forces and moments acting on a wing or body. Although significant progress has been made in the theory of non-separated laminar and turbulent flows, existing methods have a number of deficiences which introduce serious drawbacks, when separation occurs: (a) the flow model breaks down under conditions of vanishingly-small wall shear and reversed flow: (b) they neglect the important effect of viscous-inviscid interaction induced by the boundary layer displacement thickness growth, including the attendant upstream influence; (c) very little has been done to treat the turbulent case; (d) the numerical approaches involved are usually very lengthy and expensive to run and totally impractical for use in advanced engineering design calculations and parametric studies.

As a first step toward remedying these deficiences, a new approximate three-layered theoretical flow model of boundary layer separation including viscous-inviscid interaction was conceived for the case of subsonic two dimensional steady laminar flow (see Fig. 1). In this approach, the boundary layer is split up into two appropriately-matched regions: a thin viscous sublayer region (having negligable inertia) near the wall overlaid by a thick outer layer of nearly inviscid (but highly rotational) flow. Inviscid interaction is accounted for by coupling the perturbed inviscid flow to the total displacement thickness growth of the boundary layer $\delta^*(x)$ using a linearized source distribution representation of $\delta^*(x)$. The purpose of the research project was to study the theoretical development and numerical implementation of this "triple deck" flow model concept for laminar boundary layer separation problems,

with the ultimate follow-on goal of extending it to the case of fully developed
two-dimensional turbulent flow separation.

2. PRESENT STATUS OF WORK

The proposed triple deck interactive model for laminar flow has been
completely worked out and some promising preliminary numerical results obtained,
including development of a small perturbation analysis verifying the concept of
the suggested iterative calculation approach. These results were documented
and presented in an AIAA paper last summer; a copy of this, which contains all
the details of the model analysis, is given in the Appendix.

During the remainder of last summer, the numerical feasibility of the model
for treating separated flow conditions was further established, albeit in a very
inefficient form unsuited for routine applications. Subsequently, working at
a very low level of effort owing to a lack of student programmer time, we have
been slowly developing a far more efficient algorithm to implement the inter-
active model.

DISTURBED INVISCID FLOW

EDGE OF BOUNDARY LAYER $\delta(x)$

ROTATIONAL
INVISCID FLOW

$y = y_j(x)$

EQUILIBRIUM
VISCOUS SUBLAYER

y

BODY

x_0

x
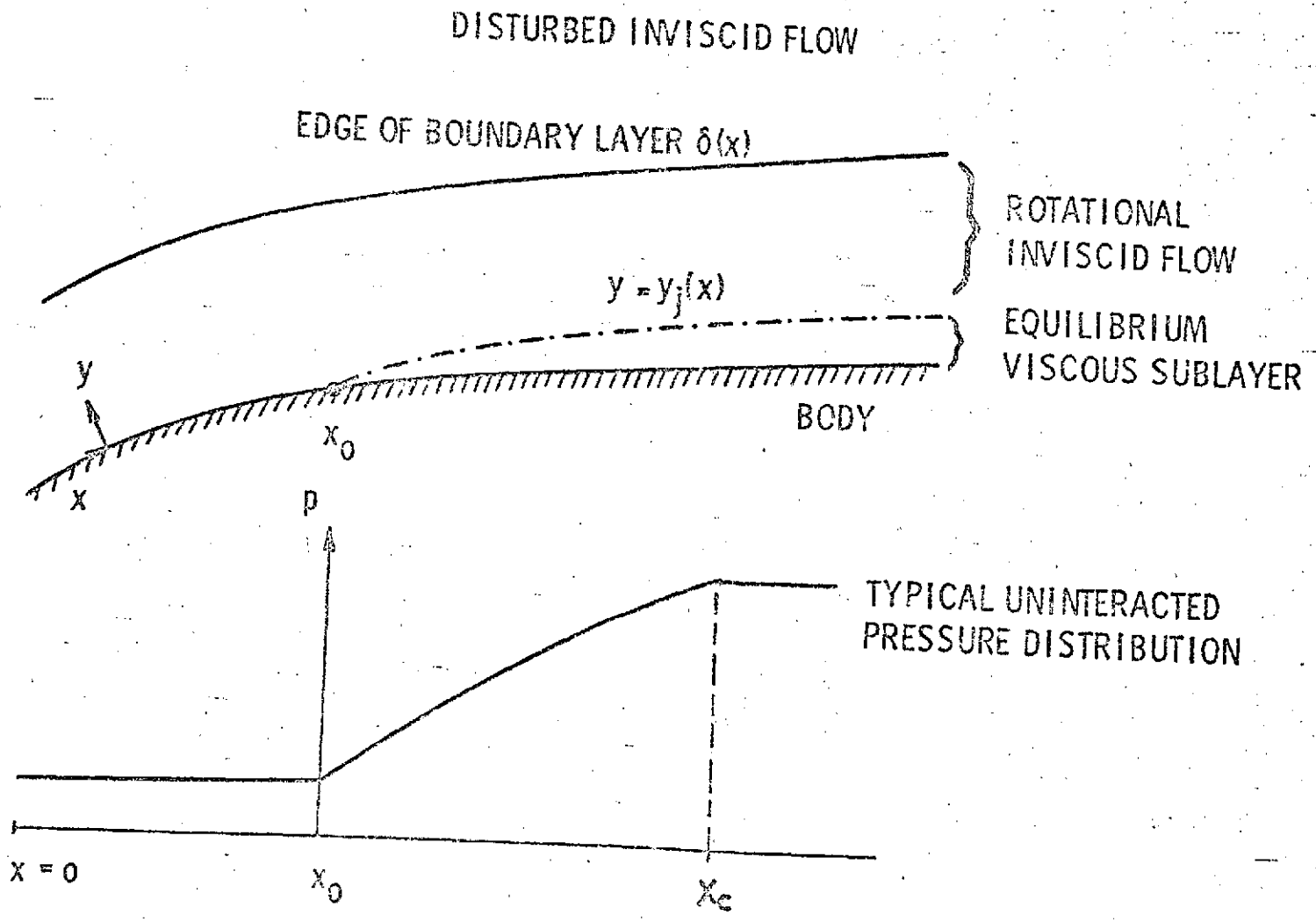
p

TYPICAL UNINTERACTED
PRESSURE DISTRIBUTION

$x = 0$

x_0

x_c

Fig. 1: Schematic of Three Layered Flow Model

APPENDIX

SUBSONIC LAMINAR BOUNDARY LAYER SEPARATION AND REATTACHMENT

WITH VISCOUS - INVISCID INTERACTION

by

G. R. Inger

Virginia Polytechnic Institute & State University
Blacksburg, Virginia   24061

Presented to

$\sqrt{i}$

SUBSONIC LAMINAR BOUNDARY LAYER SEPARATION

AND REATTACHMENT WITH VISCOUS-INVISCID INTERACTION*

Abstract

A theory is developed for nonsimilar laminar boundary layers with separation, reversed flow and reattachment including global subsonic viscous-inviscid interaction and upstream influence with application to separation bubble problems. The approach is based on an approximate triple-deck flow analysis which provides a unified, non-singular analytical model over a wide range of both attached and reversed flow states. The displacement effect on the inviscid flow is represented by a thin airfoil integral with a leading edge correction by Lighthill's rule. A closed form solution of this model is given which shows the essential features of the problem and supports the numerical approach. A global iteration calculation method is devised which is free from the usual Crocco-Lees critical points occuring in interaction problems. Application to the case of a linearly-decelerating basic inviscid flow is discussed including some preliminary numerical results.

NOMENCLATURE

a	Parameter related to inner layer thickness
c	Characteristic length
C_p	$2(p-p_0)/\rho u_{e_0}^2 = 1-(u_e/u_{e_0})^2$
C_f	$2\tau/\rho u_{e_0}^2$
N	Parameter in inner layer solution
p	Static pressure
$Re_{x,c}$	$\rho u_{e_0} x/\mu, \; \rho u_{e_0} \mathcal{L}/\mu$
T	τ/τ_B
u	Velocity component along x
v	Velocity component along y (normal to surface)
x,y	Coordinates along and normal to surface, respectively, with $x = \bar{x}/\mathcal{L}$ being non-dimensional.
δ	Boundary layer thickness
δ_B	Local Blasius thickness $= 5.2\sqrt{x}/(1-C_{p,basic})^{1/4} \, Re_c^{1/2}$
$\delta*$	Displacement thickness
δ_B*	$1.73\sqrt{x}/(1-C_{p,basic})^{1/4} \, Re_c^{1/2}$
$\theta*$	Momentum thickness
μ	Coefficient of viscosity
ψ	Stream function, location of streamline
ρ	Density
ν	Kinematic viscosity
τ	Wall shear stress $= \mu(\partial u/\partial y)_w$
τ_B	Local flat plate value $= .332\rho u_{e_0}^2 (1-C_{p,basic})^{3/4} Re_x^{-1/2}$

Subscripts

basic	prescribed non-interacted pressure distribution values
B	Local Blasius (flat plate) value

C	Cut-off point of basic pressure gradient
F	End of Interaction Region
j	Location of inner-outer layer interface
L	Effective flat plate origin for favorable initial pressure gradient
T	Effective flat plate origin for downstream of interaction
m	Maximum u_e station
o	Start of adverse pressure gradient
sep	Separation point
i	Start of interaction
w	Conditions at wall

inviscid (but highly rotational) flow. Inviscid interaction is accounted for by coupling the perturbed inviscid potential flow outside the boundary layer to the displacement thickness growth $\delta^*(x)$. There are several reasons for our selection of this approach. First, in the absence of viscous interaction effects the two-deck boundary layer model has been found to give very accurate predictions of both laminar and turbulent boundary layer behavior in adverse pressure gradients up to separation for a wide variety of flows including those with surface mass transfer.[6] Hence its extension to include interaction, upstream influence and separated flow would provide a valuable and relatively inexpensive tool for making engineering analyses of separating flow. Second, our three-layer model approach is strongly suggested by the recent investigation of Stewartson and Williams,[7] who show that the asymptotic structure of incipiently-separating laminar boundary layer flow at high Reynolds numbers does indeed have such a triple-deck character. Third, the relative simplicity of the analysis provides a clear insight to all the essential features and difficulties of the separation problem and lends itself to very straight-foreward and inexpensive numerical implementation.

In Section 2 the basic simplifying assumptions, the analytical formulation and the salient features of the model are described. It is shown that the model has a heretofore-unrecognized double-branched solution character that enables it to pass through separation and reattachment without singularities and provide a unified description of a wide range of both attached and separated flow states. Section 3 outlines a closed form method of solution which displays all the essential features of the problem and which also supports our subsequent numerical approach. In Section 4, a global iteration technique of applying this model to the numerical calculation of subsonic viscous-inviscid interaction problems in adverse pressure gradients including

2

separation is then discussed, including some preliminary results for separation bubbles occuring in a linearly-decelerating basic inviscid flow. We conclude in Section 5 with a brief discussion of further improvements and extensions of the present theory.

2. FORMULATION OF ANALYSIS

Assumptions

We first introduce a number of basic simplifying assumptions. a) As a convenient idealization to illustrate the essential features of our approach, the flow is assumed two-dimensional and steady (neither of which is strictly true in practice)[3,8] and incompressible, although the present theory can be readily extended to compressible subsonic transonic or supersonic flow including heat transfer. b) The usual high Reynolds number boundary layer-type approximations are adopted including the neglect of second order curvature effects. While this is not strictly valid near separation and reattachment points, it does not give significant errors unless the "fine structure" of the flow around these points is of interest. Indeed, the recent studies of Lees and Kleinburg,[9] Stewartson,[7,10] and Werle and Davis[11] have all shown that the use of boundary layer equations to predict separating flows is acceptable provided the pressure distribution is determined by viscous-inviscid interaction and the separation bubble region is thin. c) The flow is assumed to be laminar which is an idealization to illustrate the basic features of the analytical method and of course is of practical interest for low Reynolds number cases. The resulting analysis appears readily extendable to the turbulent case with the use of a suitable eddy viscosity model, since the essential physical features of the approach are independent of the details of the viscosity law. d) The global viscous-inviscid interaction is described by

3

coupling the perturbed inviscid flow to the boundary layer by means of a small disturbance source distribution ("thin airfoil") model of the displacement thickness effect, thereby including consideration of the upstream influence of downstream events (such as reattachment)*. (e) The types of flow considered here are those in which the basic non-interacting pressure distribution $C_{p,basic}$ is zero in the region $0 \leq x \leq x_o$ followed by an arbitrary but finite length of continuous pressure rise over $x_c \leq x \leq x_o$, see Fig. 1 (this zero pressure gradient condition for $x < x_o$ will be subsequently relaxed as discussed below. In the constant $C_{p,basic}$ region downstream of this cutoff point x_c, the boundary layer is assumed to approach a flat plate behavior appropriate to this new pressure level. Although in the present study we emphasize the case of reattaching laminar separation bubbles, the general approach is also applicable to other types of downstream boundary conditions such as those pertaining to a wake.

Flow Model-Governing Equations

Following the earlier ideas of Von Karman and Millikan as improved by Stratford and Curle, and more recently justified by Stewartsons asymptotic analyses of viscous interaction effects, the flow into an adverse pressure gradient region can be divided into three essential layers (see Fig. 1). The viscous boundary layer region for $x > x_o$ is divided into two strata: a thin "local equilibrium" sublayer $0 \leq y \leq y_j$ near the surface where inertia effects are negligible, overlaid by a thick outer layer of essentially inviscid but rotational flow with a small viscous total head loss that is conveniently

---

* A vortex sheet model could also be used; in fact the present boundary layer model can be mated to any suitable numerical potential flow program (such as Hess and Smith[12]).

4

approximated by a local flat plate value. The third layer is the disturbed

outer inviscid flow which globally interacts with the boundary layer. Since

the analytical formulation of this two-layered boundary layer model has already

been discussed in detail by several authors,[5,6] only a brief outline need be given

here with emphasis on the new features not considered heretofore.

Regarding the thick nearly-inviscid rotational outer flow layer $y \geq y_j$

the velocity along any streamline x, ψ is approximated by the variable total

head Bernouli equation

$$[u^2]_{x,\psi} \simeq [u_B^2]_{x,\psi} - \frac{2(p-p_o)}{\rho} \tag{1}$$

where u_B is the <u>local</u> flat plate (Blasius) solution pertaining to $C_{p,basic}$

which approximately accounts for the viscous total head loss along the stream-

line. Successive differentiations of Eq. (1) with respect to ψ and neglecting

the lateral pressure gradient yields the two equations

$$\left(\frac{\partial u}{\partial y}\right)_{x,\psi} = \left(\frac{\partial u_B}{\partial y}\right)_{x,\psi} \tag{2}$$

$$\left(\frac{\partial^2 u}{\partial y^2}\right)_{x,\psi} = \frac{u}{u_B}\left(\frac{\partial^2 u_B}{\partial y^2}\right)_{x,\psi} \tag{3}$$

The flow in the thin inner layer $0 \leq y \leq y_j(x)$ has negligible inertia and

lateral pressure gradient $(p_w \simeq p_j)$ and following Curle[6] may be described

by the following velocity profile which satisfies the momentum Eqn. as

$y \rightarrow 0$:

$$u = \tau y/\mu + (dp/dx) y^2/2\mu + a(x) y^N/\mu \tag{4}$$

5

where $\tau = \mu(\partial u/\partial y)_w$ is the wall shear stress, the function a(x) is related to the unknown value of y_j as determined by matching with the outer solution, and N is an arbitrary parameter with $N \geq 3$. The two layers are matched by requiring that ψ, u, $\partial u/\partial y$ and $\partial^2 u/\partial y^2$ each be continuous at $y = y_j$, these conditions being sufficient to determine τ, a(x), y_j and ψ_j with N appearing as an arbitrary profile parameter (the value N = 3.043 recommended by Curle[6] for unseparated non-interacting flows in adverse pressure gradients is used here without change). As in Stratford's original work,[5] the inner layer is presumed to lie within the linear region of the Blasius profile; consequently the aforementioned inner-outer matching yields the following approximate analytical relationship between the skin-friction and surface pressure distribution:

$$x^2 C_p \left(dC_p/dx\right)^2 = .0122 \ (1-T)^3 \left[1 + \frac{3(N^2-1)}{(N^2+3)} \ T\right] \left[\frac{(N-1)^3 (N^2+3)}{3N^2 (N+1)(N-2)^2}\right] \qquad (5a)$$

$$= .0104 \ (1-T)^3 (1+2.02T) \qquad \text{for N = 3.04} \qquad (5b)$$

where $T \equiv \tau/\tau_B$ with $\tau_B \simeq .332 \ \rho u_{eo}^2 \ (1-C_{p,basic})^{3/4} \ Re_x^{-1/2}$. It is emphasized that this relation is perfectly general as regards the nature of the pressure field; it refers either to a prescribed or freely-interacting $C_p(x)$.

Although Curle has shown that the assumption $u_B \simeq \tau_B \ y/\mu$ in the inner layer limits the pressure coefficient to values less than about 0.11, both his results and our own calculations indicate that accurate predictions of separation from Eq. (5) may still be obtained for values of pressure coefficient at separation as high as 0.25. Moreover, since viscous-inviscid interaction further reduces the pressure level near separation (see below), this limitation

6

on Eq. 5 is not an important one in the present study. A more significant

limitation stems from the neglect of the inertia effect (flow history) of the

inner layer; Eq. (5) consequently preducts that $\tau = \tau_B$ wherever the local

pressure gradient vanishes, which certainly yields inaccurate results for

prescribed pressure distributions with maxima or minima or for viscous-inviscid

interactions involving local overshoots in the pressure.

The unknown inner layer thickness is given by the aforementioned matching

as

$$y_j = \frac{N-1}{N-2} \left[\frac{(1-T)C_{f,B}}{dC_p/dx} \right] \tag{6}$$

with a limiting value of zero as the pressure gradient vanishes. The corre-

sponding total boundary layer displacement thickness is composed of contribu-

tions from the inner and outer layer regions as follows:

$$\delta^* = \int_0^{y_j} \left(1 - \frac{u_{inner}}{u_e}\right) dy + \int_{y_j}^{\delta} \left(1 - \frac{u_{outer}}{u_e}\right) dy \tag{7a}$$

where δ is the effective edge of the boundary layer (Appendix A). The dominant

contribution to the displacement thickness is from the inner layer. Using

Eqs. (1), (4) and (6), Eq. (7a) becomes

$$\delta^* = y_j \left[1 - \frac{y_j(1+T)}{2\delta_B} \right] + \delta \int_{y_j}^{\delta} \left[1 - \sqrt{\left(\frac{u_B}{u_e}\right)^2 - \left[C_p/(1-C_p)\right]} \right] dy \tag{7b}$$

As shown in Appendix A, this can be approximated by the following expression

which proves useful later:

$$\delta^* \simeq \delta_B{}^* + \delta - \delta_B + \frac{y_j{}^2}{2\delta_B} (1-T) \qquad (7c)$$

which correctly passes over to the result $\delta^* \to \delta_B{}^*$ in the absence of pressure

gradient $(y_j \to 0)$ where δ_B and $\delta_B{}^*$ are the local flat plate displacement thick-

nesses.

The effect of the global interaction between the boundary layer and the

external inviscid flow is treated by correcting the original potential flow

for the total boundary layer displacement effect following the approach pre-

viously used successfully by a number of investigators, in which the velocity

field perturbation due to the displacement thickness is represented by an

equivalent source-sink distribution. Thus, for example, using the small dis-

turbance approximation to Bernouli's equation and evaluating the source-sink

distribution effect at $y = \delta^*$ as recommended by Preston[13] (who found that

this gave good agreement with experiment for airfoil calculations), the in-

teracting pressure field can be expressed as $C_p = C_{p,basic} + \Delta C_p$ where

$$\Delta C_p = \frac{-2}{\pi} \sqrt{1-C_{p,basic}} \int_0^\infty \frac{(x-\xi)\frac{d\delta^*}{dx}(\xi)d\xi}{(x-\xi)^2 + \delta^*(x)^2} \qquad (8a)$$

is the local correction to the prescribed basic (non-interacting) pressure due

to the entire displacement thickness with ξ the dummy variable of integration.

Note that the integral is not singular at the source point $\xi = x$, which is

advantageous in the numerical work. As shown in Appendix B, examination of the

limits and integration by parts enables Eq. 8a to be expressed for computational

purposes in the form

$$\Delta C_p \simeq -\frac{2\sqrt{1-C_{p,basic}}}{\pi}\left\{\left[\frac{\delta^*\cdot(x-\xi)}{(x-\xi)^2+\delta^{*2}}\right]_{x_i}^{x_f} - \int_{x_i}^{x_f}\frac{[(x-\xi)^2-\delta^{*2}]\delta^*}{[(x-\xi)^2+\delta^{*2}]^2}d\xi\right\} \tag{8b}$$

where $x_i \to 0$ and x_f are the effective start and end, respectively, of the viscous-inviscid interaction region with $x_f \gg x_c$. Alternatively, using the classical "thin airfoil integral" formulation of ΔC_p in which the source-sink effect is evaluated along $y = 0$ instead of $y = \delta^*$ with the resulting leading edge singularity eliminated by the so-called Lighthill rule correction factor[14], Eq. (8a) reduces to the following well-known singular integral equation requiring the use of the Cauchy principal value at $x = \xi$:

$$\Delta C_p \simeq -\frac{2}{\pi}\sqrt{(1-C_{p,basic})\left(\frac{x}{x+r_0}\right)}\int_0^\infty \frac{(d\delta^*/\delta x)d\xi}{x-\xi} \tag{8c}$$

where $r_0 = (\delta_B^{*2}/2x)_{x\to 0} = 1.5\,Re_c^{-1} = 1.5\varepsilon^2$. Excluding the small higher order region of size r_0 near the leading edge, this integral has the important property of vanishing identically for the flat plate parabolic distribution $\delta^* = \delta_B^* \sim \sqrt{x}$ [†]; hence from Eq. 7C we see that only the pressure gradient effect on δ^* effectively contributes to the viscous interaction-induced pressure field.

Important Features Pertaining to Separation

For illustrative purposes, we consider the case of linearly-retarded flow $u_e/u_0 = (1-x)$ $[C_{p,basic} = (2-x)x]$ for which an exact solution of the boundary layer equations has been obtained by Howarth.[15] The resulting solution of Eq. (5) for the shear stress distribution along the wall is shown in Fig. 2. From this Figure we can perceive several important features of the present approach.

[†]This result may be understood from the fact that there is no pressure gradient immediately downstream of the nose of a parabola in incompressible flow.

First, we see that the two-layer boundary layer model is in excellent agreement with the exact solution, giving an accurate account of the decrease in skin friction up to separation including the location of separation itself around $x_{sep} \cong .12$. Actually, the two-layer result continues slightly downstream of this x_{sep} corresponding to a small reversed flow (further comment on this is given below).

Second, it is observed in Fig. 2 that the solution is double-valued: for each value of x and C_p one obtains <u>two</u> values of shear stress, one positive and one negative, corresponding to attached and reversed flows, respectively (note that Eq. 5b is a quartic in T with either a pair of real and a pair of imaginary roots or two pairs of imaginary roots). Moreover the upper and lower "branches" of this solution are seen to be continuously connected. This heretofore-overlooked double-valued nature of the two-layer boundary layer model is analogous to the well-known double-branched similarity solutions of the boundary layer equations for negative values of the pressure gradient para-meter.[16] Now, such a feature endows the present analytical approach with the inherent capability of giving a unified continuously-connected description of both attached and full-separated flow states <u>provided</u> we "unhook" the pressure field in the skin friction-pressure relation from a prescribed explicit de-pendence on x and instead allow it to be coupled to the boundary layer by viscous-inviscid interaction.* Thus, by interpreting Eq. 5 or Fig. 2 as a τ vs. C_p locus (instead of τ vs. x) the physical solution can move along AB with an increasing pressure toward separation, then from the upper to the lower branch through separation into a separated flow region along BC with

---

* In the same manner as Lees and Reeves[17] employed self-similar boundary layer solutions in supersonic viscous-inviscid interaction problems by "unhooking" them from the pressure gradient parameter.

decreasing interaction pressure, then back along CB through rising pressure toward reattachment and through reattachment followed by downstream post-reattachment relaxation with decreasing pressure along BA.

Third, it is important to note that unlike previous solutions of the full boundary layer equations, the approximate two-layer boundary layer model does not give a singularity at the separation point; this is evident in Fig. 2, where the slope of the wall shear stress at separation $(d\tau/dx)_{sep}$ is seen to be finite (this can be also be verified by direct differentiation of Eq. 5 with respect to x).[†] Interestingly enough, this result is in qualitative agreement with experimental data and the predictions of exact numerical solutions of the Navier-Stokes equations in adverse pressure gradients[18-20], both of which indicate that $d\tau/dx$ is finite (though large) as $\tau \to 0$. Lee[21] has shown in fact that the usual boundary layer solutions[28] giving a separation point singularity are not valid in the immediate vicinity of x_{sep}; when this is corrected, a regular behavior through separation is obtained. Indeed, he further shows by an asymptotic analysis of the Navier-Stokes equations near x_{sep} that to the leading order of approximation the viscous flow near the surface is described by precisely the inner layer flow model used herein. Additional support for at least the approximate correctness of the present model on this point can be obtained by examining the zero streamline $\psi = 0$ whose locus indicates where the flow separates from the surface: integrating the inner velocity profile Eq. (4) with respect to y and using the matching relations, this locus is found to be governed by $y_{\psi=0} = 0$ for $\tau > 0$ and in a reversed flow region by the relation

---

[†] The behavior near separation does not depend sensitively on N; for example, the cube root of the right side of Eq. 5 evaluated at $\tau = 0$ (which is approximately proportional to x_{sep} for linearly-retarded flow) decreases by only 16% when N is changed from 3 to 4.

$$3 T \mathcal{C}_{f,B} + \frac{dC_p}{dx} \left[y - \frac{6y^{N-1}}{N(N^2-1)y_j^{N-2}} \right]_{\psi=0} = 0 \qquad (9)$$

Differentiating this with respect to x and setting $y_{\psi=0} = 0$ at $\tau = 0$, Eq. (9) predicts that the separation streamline leaves the surface at a finite angle γ given by

$$\tan\gamma = \left(\frac{dy_{\psi=0}}{dx} \right)_{sep} = -3 \left(\frac{d\tau/dx}{dp/dx} \right)_{sep} \qquad (10)$$

which under the assumption dp/dy = 0 is in exact agreement with the well-known value derived from the full Navier-Stokes equations by Oswatitsch.[22] Both separation and reattachment occur in a non-singular manner at a well-defined acute angle to the surface.

Aside from Fig. 2., a fourth noteworthy aspect of the present analysis is the relative structure of the flow in a separation region predicted by the inner layer flow model. Thus, in addition to the aforementioned zero streamline, the zero velocity locus that delineates the extent of the reversed flow region is found Eq. (4) to be governed by

$$2 T \mathcal{C}_{f,B} + \frac{dC_p}{dx} \left[y - \frac{2}{N(N-1)} \times \frac{y^{N-1}}{y_j^{N-2}} \right]_{u=0} = 0 \qquad (11)$$

In addition the conesponding zero velocity gradient locus ($\partial u/\partial y = 0$) where the maximum reversed flow speed occurs is given by

$$T \mathcal{C}_{f,B} + \frac{dC_p}{dx} \left[y - (N-1) \times \frac{y^{N-1}}{y_j^{N-2}} \right]_{\frac{\partial u}{\partial y} = 0} = 0 \qquad (12)$$

12

Since these locii derive from the inner layer solution, they must all lie within $0 \le y \le y_j$ and this is indeed readily verified to be the case by comparing Eq. (6). Moreover, Eqs. (19), (11) and (12) predict that the ordinates $(y)_{\psi=0}$, $(y)_{u=0}$ and $(y)_{\partial u/\partial y=0}$ are approximately in the ratio 3:2:1 independent of N; this agrees with the relative size of these ordinates shown in Leal's Navier-Stokes solutions.[20]

Fifth, it should be noted that governing model equations automatically yield the correct downstream solution [namely a flat plate boundary layer corresponding to $C_{p,basic}$ (x_c)] far downstream where the pressure gradient vanishes; for when $dC_p/dx \to 0$ with $x \gg x_c$, Eqs. 5 and 6 give $T \to 1$, $y_j \to 0$ while Eqs. (7) yields the correct corresponding displacement thickness.

Sixth, shown in Appendix B the displacement thickness integral in Eq. 8b has the important property of becoming vanishing small (with a concomittantly-vanishing x-derivative) at both $x = x_i$ and $x = x_f$ provided x_i and x_f are chosen sufficiently small and large, respectively. Consequently, the inter-action-induced pressure ΔC_p and its streamwise gradient and hence (by Eqs. 5 and 7) the corresponding shear and displacement perturbations all automatically vanish at x_i and x_f to any desired degree of accuracy.

Allowance for an Initial Pressure Gradient

The foregoing analysis can be extended to include boundary layer flows with a non-zero upstream favorable pressure gradient history in the region $0 \le x \le x_0$ by adapting the equivalent flat plate initial condition technique of Curle.[6] Thus if the inviscid flow velocity distribution $u_e(x)$ increases to a maximum u_{e_m} at the pressure minimum station $x = x_m$, the boundary layer velocity profile at x_m will be very similar to a Blasius profile based on some equivalent length $x_m - x_L$ if the equivalent origin x_L is determined by

requiring the same momentum thickness $\theta*$ at x_m. Equating $\theta*^2 = \mathcal{V} u_{e_m}^{-6} \int_0^{x_m} \cdots$ $u_e^5 dx$ given by the accurate Thwaites method[23] to the equivalent flat plate value $.45 \, \mathcal{V} u_{e_m} (x_m - x_L)$ yields

$$x_L = x_m - \int_0^{x_m} \left(u_e / u_{e_m}\right)^5 dx \qquad (13)$$

The subsquent boundary layer development in the adverse pressure gradient region may then be treated by the foregoing model provided x is replaced by $\bar{x} = x - x_L$ and the skin friction and the pressure coefficient are defined in terms of conditions at x_m instead of x_o.

The above equivalent origin approach can also be used to partially account for the "memory" effect of the upstream adverse pressure gradient history on the far downstream post-reattachment conditions in the case of the viscous-inviscid interaction separation bubble problem, as discussed below.

3. ANALYTICAL SOLUTION

An analytical solution of the foregoing theoretical flow model can be obtained which is a very helpful guide in constructing our numerical approach. To bring out the essential ideas involved, we adopt the approximate displacement thickness expression (7c) and neglect the $\delta*^2$ term in the integrand denominator of Eq. (8) [neither of these simplifications alters the basic correctness of the subsequent analysis]; then using the values of δ and y_j given by Appendix A and Eq. (6), respectively, and noting that $\delta_B* \simeq 1.73 \, x^{1/2} \varepsilon$ $(1 - C_{p,basic})^{-1/4}$ where $\varepsilon \equiv Re^{-1/2}$, we obtain from Eqs. (5b), (7c) and (8) the following trio of equations that characterize our interacting triple-deck flow model:

$$x^2(dC_p/dx)^2 C_p = .0104 \ (1+2.02T)(1-T)^3 \qquad (14)$$

$$C_p = C_{p,basic} - \frac{2}{\pi} \sqrt{1-C_{p,basic}} \int_0^\infty \frac{(d\delta*/dx)d\xi}{x-\xi} \qquad (15)$$

$$\delta* \simeq \varepsilon \frac{\sqrt{x}}{(1-C_p)^{1/4}} \left\{ 1.73 + \left(\frac{\delta-\delta_B}{\delta_B*}\right) + \frac{.086(1-T)^3(1-C_p)^2}{(x \ dC_p/dx)^2} \right\} = \varepsilon \ d(x) \qquad (16)$$

Eq. (14) characterizes the overall pressure-shear force balance of the boundary layer while Eq. (15) introduces the global effect of the displacement thickness growth on the pressure distribution in subsonic flow, as well as containing the "basic" non-interacting pressure distribution that characterizes the particular problem at hand.

The trio (14)-(16) in general constitutes a difficult integro-differential equation system to be solved for the three unknowns T, C_p and $\delta*$. However, the presence of the parameter ε and the fact that it is very small under precisely the high Reynolds number conditions appropriate to the present model suggests that a perturbation approach is feasible[†] in which the solution is expanded in ascending powers of ε, as follows:

$$C_p = C_{p,basic} + \varepsilon \ \Delta C_{p1} + \varepsilon^2 \Delta C_{p2} + \ldots \qquad (17a)$$

$$T = T_{basic} + \varepsilon \ T_1 + \varepsilon^2 T_2 + \ldots \qquad (17b)$$

$$\delta* = \varepsilon \ d_{basic} + \varepsilon^2 d_1 + \ldots \qquad (17c)$$

[†] A similar approach was successfuly used by Ting[24] to solve a massive blowing problem having an analogous mathematical structure to the present one.

That is, since the displacement effect (within the accuracy of the boundary layer approximation) and hence the induced pressure are everywhere of small order ε, the leading approximation is the non-interacting solution; the small (order ε) first interactive "correction" to this is obtained in terms of the $\delta*$ for the "basic" flow. Thus, for example, substitution of expansions (17) into Eqs. (14)-(17) yield to first order that

$$\Delta C_{p1} = -\frac{2}{\pi}\sqrt{1-C_{p,basic}} \int_0^\infty \frac{[d(d_{basic})/dx]}{x-\xi} d\xi \qquad (18)$$

$$T_1 = -\frac{(1-T_{basic})(1+2.02\ T_{basic})}{-3-2.02(1-4\ T_{basic})} \left[\frac{\Delta C_{p1}}{C_{p,basic}} + 2\frac{d\Delta C_{p1}/dx}{dC_{p,basic}/dx} \right]$$

$$(19)$$

with analogous expressions for ΔC_{p2} (involving an integral of d d_1/dx) and T_2, etc.[†] This procedure has thus converted the original problem involving an integral equation into a succession of quadratures of known displacement thickness functions.

It is pointed out that the "basic" solution appearing in the foregoing analysis can be approximated by any reasonable distribution without altering the essential correctness or accuracy of the analysis, at least to first order in the interaction effects. Consequently, in the case where separation would occur in the basic flow, we may use an intelligent non-singular projective estimate of the $\delta*$ distribution across the length of the reversed flow in evaluating Eqs. (18) and (19). In this manner, our analytical solution provides the suggestion of (and support for) the streamwise-pass iterative method of numerical solution discussed in the next section.

[†]It is understood that $\varepsilon \ln \varepsilon$ type terms may intervene between ε and ε^2 in Eqs. (17).

4. NUMERICAL SOLUTION SCHEME

Global Iteration Approach

We have seen in Section 2 that the present triple-deck flow model has the inherent capability of giving a unified, continuously-connected description of both attached and fully-separated flow states provided we "unhook" the pressure field in the skin friction-pressure relation from a prescribed explicit dependence on x and instead allow it to be coupled to the boundary layer by global viscous-inviscid interaction. The resulting solution can be thought of as being defined by the intersection of two locii (see Fig. 3): the locus of all possible shear vs. pressure gradient values for the boundary layer as defined by Eq. 5, and the "interaction" locii of T vs. pressure at various x implied by the integral of $\delta^*(T, C_p)$ in Eq. 8. The numerical solution of this problem is a difficult one since inclusion of the global subsonic interaction makes the problem quasi-elliptic and hence introduces the need to impose downstream boundary conditions. However, the discussion in Section 3 suggests that the most expedient approach is to use a global iteration method involving successively-refined streamwise passes. A very similar type of scheme has been proposed recently by Lees and Su for solving a stratified flow separation problem[25] and by Jobe and Burggraf for interacting trailing edge flow.[26]

The manner of implementing this approach is as follows. Starting with a prescribed basic pressure distribution (which defines the specific problem), the complete non-interactive solution is calculated along the body, stopping in the event of incipient separation at some station $x = x_1$ slightly upstream of the separation point. Following Catherall and Mangler[27] we then project from this station a first estimate of the downstream behavior of δ^* throughout the entire interaction zone assuming a regular continuous behavior; specifically,

17

we used a cubic polynominal projection $\delta^* = \delta^* (x_1) + a_1(x-x_1) + a_2(x-x_1)^2 + a_3(x-x_1)^3$ where $a_1 = (d\delta^*/dx)_{x_1}$ while a_2 and a_3 are determined by requiring that δ^* and $d\delta^*/dx$ be equal to local flat plate values at some first guess of the downstream interaction-termination distance x_f. Having such a reasonably-behaved first approximation for $\delta^*(x)$ over the entire flow length, one can make a corresponding smoothed first estimate of the displacement effect ΔC_{pl} on the pressure distribution and thereby provide a basis for performing another streamwise pass in which the viscous-inviscid interaction is now included. According to our analytical solution (Eq. 17) and previous discussion, the results so obtained for T. and $C_p = C_{p,basic} + \Delta C_{pl}$ should in fact be a fairly good first approximation to the final correct interactive values when the Reynolds number is large, provided x_f has been chosen sufficiently large.

The second streamwise pass through is begun at some suitably small value of the upstream interaction-starting point x_1. Retaining the aforementioned first guess for x_f the numerically-smoothed, interaction-modified pressure distribution $C_{pl} = C_{p,basic} + (\Delta C_p)_1$ (where subscript 1 denotes the first iteration) is used in Eq. (5b) to obtain an improved estimate of the skin friction distribution. Separation and penetration into the reversed flow region may now be allowed along the negative τ branch of the τ vs. C_p curve (such as segment BC in Fig. 2); as the flow proceeds downstream the effect of interaction dies down and the solution moves back through reattachment, relaxing toward a local flat plate behavior at the constant $C_{p,basic}(x_c)$ until finally the interaction effectively ceases at the downstream location x_f. Correspondingly, a new corrected displacement thickness distribution can be calculated directly from Eq. 7 (the polynomial projection now being discarded) and hence an improved interaction pressure correction $(\Delta C_p)_2$ for the second streamwise pass, and so

18

on. The modified pressure distribution for this second and all subsequent passes may be calculated by correcting the previous result, avoiding further direct use of $C_{p,basic}(x)$; thus for the n-th iteration with $n \geq 2$, $C_{p,n}(x) = C_{p,n-1}(x) + (\Delta C_{p,n} - \Delta C_{p,n-1})$. These iterative streamwise passes are carried out until the solution no longer changes to within a specified amount. In general, the resulting skin friction and local pressure may not agree sufficiently with the desired downstream boundary conditions appropriate to the particular problem, implying that the original estimate of x_f was too small. A series of larger x_f values are then used, each accompanied by the aforementioned sequence of streamwise pass calculations, until the downstream boundary conditions of vanishing ΔC_p and dC_p/dx are satisfied to within the desired degree of accuracy.

There are several aspects of the aforementioned numerical scheme that should be noted. (a) Owing to T and ΔC_p being defined in reference to the local basic flow, and the previously-noted property of Eq. 8 that both ΔC_p and $d\Delta C_p/dx$ can be made vanishingly small at a large and small enough $x = x_f$ and x_i, respectively, it is seen that each streamwise pass inherently satisfies the correct initial and downstream conditions. In other words, our formulation insures that every iteration is automatically "tied down" to the proper non-interactive end points that define the basic problem. (b) In view of the experience of Jobe and Burgraf[26] and others,[29] convergence of the aforementioned iteration process may be difficult to achieve without the use of "under-relaxation," in which only a fraction (usually half or less) of the correction to $\delta*$ is fed back to obtain a new interacted pressure. A schematic illustration of the proposed global iteration procedure involving 80% under-relaxation is shown in Fig. 4. (c) It is important to note that the present solution

method does not encounter any Crocco-Lees throat-type singularity. This is due to the fact that we do not handle the viscous-inviscid interaction as an initial value problem (which Garvine[30] has shown always leads to such a downstream singularity) but instead as an effective boundary value problem: our n-th iterative calculation of the interacting flow is always based on the known $\delta^*(x)$ and $C_p(x)$ distributions throughout the flow pertaining to the previous n-1 streamwise pass, with the first streamwise projection done in the manner of Catherall and Mangler.[27] Shamroth and McDonald[31] have also shown that this approach provides an adequate treatment of upstream influence effects and downstream boundary conditions without introducing streamwise saddle point-type singularities. (d) In carrying out the solution, it is possible to further improve our treatment of the post-reattachment flow by incorporating a correction to the effective origin seen by the flow due to its' upstream adverse pressure gradient history. Thus, while in the case of an initial favorable pressure gradient the flow quickly forgets its history, the thickening and separation of the boundary layer associated with the traversal of an unfavorable pressure gradient region is not so readily forgotten even by the flow well downstream of reattachment. Hence the velocity profile at the interaction-cessation point x_f will have a Blasius shape but with flat plate displacement thickness and skin friction values based not on x_f but instead on $x_f + x_T$ where x_T is some effective origin shift accounting for the upstream adverse pressure gradient history. Owing to the neglect of pressure gradient effects on the head loss in the outer layer (Eq. 1), the present theory does not include this memory effect. However, x_T can be estimated from the equivalent momentum thickness technique described in Section 2. Thus we obtain

$$x_T + x_f \approx \int_0^{x_f} \left(\frac{u_e}{u_{e,o}} \right)^5 dx \qquad (20)$$

where as a first approximation in evaluating the integral, the viscous-inviscid interaction effect on the $u_e(x)$ history has been neglected, i.e., we have used the given basic inviscid flow solution for u_e.

Some Preliminary Results

An attractive basic flow for theortical studies of separation is the special case of Howarth's linearly-decelerating flow[15] in which the basic adverse pressure gradient is applied right from the leading edge [that is, there is no boundary layer preceeding the pressure rise: $x_o = 0$, $\delta*(x_o) = 0$]. By cutting off this basic pressure gradient, reattachment and various finite lengths of separation bubble flow can be created (Briley[19] has obtained some exact numeri-cal solutions of the Navier-Stokes equations for several such cases which we also shall consider). The downstream boundary conditions appropriate to this class of flows are that the flow attain an appropriate local zero pressure gradient with Blasius skin friction behavior at some distance x_f downstream following reattachment where interaction ceases.

The present investigation has been addressed to the specific examples of linearly-decelerating inviscid flow considered by Briley[19] involving two dif-ferent lengths of basic adverse pressure gradient, one of which causes separa-tion and one of which does not. His skin friction predictions for these cases (labeled Two and One, respectively) are illustrated in Fig. 5. It is interesting to note that whereas Howarth's boundary layer solution predicts separation for both cases, Brileys results predict separation further downstream with in fact no separation at all in Case 1. This serves to emphasize that predictions of

separation by classical boundary layer solutions neglecting viscous-inviscid interaction are not always reliable. Note also from Case 2 that both separation and reattachment occur without any singularities.

An illustration of the typical displacement thickness obtained by the polynomial-projection procedure used in the first streamwise pass of our proposed iteration method is given in Fig. 6 for Case 2. Our first streamwise-projected δ^* distributions for both Cases 1 and 2 (based on the crude first estimate $x_f \approx .50$ – see Fig. 5) are compared with Briley's results in Fig. 7. In general, it appears that this "first guess" procedure yields reasonably good results with a reasonable choice of x_f. Note that the present theory does not give quite the same value of the downstream local Blasius thickness because of its very approximate account of the upstream history effect on the effective origin.

The first interactive pressure correction ΔC_p associated with the integral of our project δ^* for Case 2 is shown in Fig. 8a. This is a rough result only, having been obtained with only a crude numerical integration routine and devoid of the Lighthill correction for the leading edge singularity. Nevertheless, when a smoothed-out curve fit of this result (shown dashed) is subsequently added to $C_{p,basic}$, the resulting first interactive pressure distribution C_{p1} (Fig. 8b) is quite reasonable: the effect of interaction has appreciably smoothed and broadened out the basic pressure distribution so as to relieve the adverse pressure gradient preceeding separation (thereby explaining why separation tends to be significantly delayed compared to classical boundary layer theory predictions). It can also be seen that this interacted pressure distribution tends to form a plateau in the separated flow region, although this tendency is not as pronounced here as it would be in supersonic flow owing to the difference in shapes that constant pressure surfaces assume in subsonic

vs. supersonic irrotational inviscid flow. Downstream, reattachment occurs through a continuous monotonic pressure rise. All these features are in general agreement with experimental observation.[32]

Our current efforts are involved with improving the original implementive techniques of the global iteration procedure (as regards a more accurate numerical evaluation of the interaction integral and incorporating underrelaxation into the iteration scheme) so as to extend the foregoing preliminary results to iteratively-converged final answers including wall shear distributions and velocity profiles along the entire length of the interaction and separated flow regions. Upon achieving this, it is then planned to run some parametric studies of the linearly-decelerating problem varying the length and shape of the adverse pressure gradient region, the value of $C_{p,basic}(x_c)$, Reynolds number, and allowing non-zero initial boundary layer thickness ($x_o > 0$). Hopefully, some cases might also be run where at least limited comparisons could be made with experimental data on airfoil leading edge laminar separation bubbles[33].

5. CONCLUSION

Although approximate the present theory has the virtues of sound physical modeling of the essential flow features including viscous-inviscid interaction and upstream influence, an analytical formulation which is readily implemented numerically, and good engineering accuracy. The triple-deck model has the inherent capability of passing smoothly through a separation point into a reversed flow region and back through a point of reattachment without singularities. In addition to providing a method for obtaining approximate engineering solutions of boundary layer separation problems, the present theory would be a useful analytical tool for simulating the process of reattachment itself by providing

suitable fully-separated shear flow configurations. Furthermore, the present theory may serve as a valuable aid in the development of more rigorous and detailed exact numerical methods for high Reynolds number flows by providing estimates of the location and mesh size requirements of the high shear and reversed flow regions. Finally, we reemphasize that the triple-deck model approach is applicable not only to flows with reattachment but also appears adaptable to those where other types of downstream condition pertain such as a wake.

Many improvements and extensions on the present analysis appear possible. For example, the assumption that the total head loss in the outer layer is not influenced by the pressure gradient can be relaxed, as can the neglect of the convective inertia effects in the inner layer (this would enable the theory to treat basic pressure distributions with maxima or minima). Extension can also be made to include compressibility effects for either subsonic, transonic or supersonic flow, including heat and mass transfer. Furthermore, it is clear from Stratford's pioneering study of the two-layer model for non-interacting incipiently-separated turbulent boundary layers[34] that the present approach can extended to interacting turbulent flows provided a suitable eddy viscosity model for the strongly-adverse pressure gradient and reversed flow regions is available. Finally, the theory can be applied to treat three dimensional flows since there is nothing inherent in the character of either the inner or outer layer approximations that cannot be extended to include the presence of a cross flow.

REFERENCES

1. Klineberg, J. M. and J. L. Steger, "On Laminar Boundary Layer Separation", AIAA Paper 74-79, Feb, 1974.

2. Carter, J. E., "Solutions for Laminar Boundary Layers with Separation and Reattachment," AIAA Paper 74-583, June, 1974.

3. Tani, I., "Low-speed Flows Involving Bubble Separations", Progress in Aeronautical Sciences, Vol. 5, edited by D. Kuechemann and L. H. G. Steme, Pergamon Press, London, 1964, pp. 70-103.

4. Von Karman, Th. and C. B. Millikan, "On the Theory of Laminar Boundary Layers Involving Separation", NACA Report 504, 1934.

5. Stratford, B. D., "Flow in the Laminar Boundary Layer Near Separation", British ARC R&M 3002, Nov. 1954.

6. Curle, N., "Estimation of Laminar Skin Friction, Including the Effects of Distributed Suction", Aero. Quart. XI, Feb. 1960, p. 1-21.

7. Stewartson, K. and P. G. Williams, "Self-Induced Separation", Proc. Roy. Soc. of London A, 312, September 1969, pp. 181-206.

8. Fricke, F. R. and Stevenson. D. C., "Pressure Fluctuations in a Separated Flow RLgion", Journal of the Acoustical Society of America, Vol. 44, No. 5, Nov. 1968, pp, 1189-1201.

9. J. Kleinburg and L. Lees. " Theory of Viscous-Inviscid Interactions in Supersonic Flow", AIAA Journal 7, 1969, pp, 2211-21.

10. Brown, S. N. and K. Stewartson, "Laminar Separation", article in Annual Review of Fluid Mechanics 1, 1969, pp, 45-72.

11. Werle, M. J. and R. T. Davis, "A Consistant Formulation of Compressible Boundary Layer Theory with Second Order Curvature and Displacement Effects", AIAA Journal 8, September 1970, pp, 1701-03.

12. Hess, J. L. and Smith, A.M.O., "Calculation of Potential Flow About Arbitrary Bodies", Progress in Aeronautical Sciences, Vol. 8. Pergamon Press, New York, 1966, p. 1-138.

13. Preston, J. H., "The Effect of the Boundary Layer and Wake on the Flow Past a Symmetrical Aerofoil at Zero Incidence", British ARC R&M No. 2207, July 1945.

14. Van Dyke, M., Perturbation Methods in Fluid Mechanics, Academic Press, New York, 1964, pp. 59-64.

15. Howarth, L., "On the Solution of the Laminar Boundary Layer Equations", Proc. Royal Soc. A., 164, 1938, p. 542.

16. Stewartson, K., "Further Solutions to the Falkner-Skan Equation", Proceedings of the Cambridge Philosophical Society Vol. 50, 1954, pp. 454-465.

17. Reeves, B. L. and L. Lees, "Supersonic Separated and Reattaching Laminar Flows, I. General Theory and Application to Adiabatic Boundary Layer/ Shock Wave Interactions", AIAA Journal 2, Nov. 1964, pp. 1907-1920.

18. Werle, M. J. and R. T. Davis, "Incompressible Laminar Boundary Layers on a Parabola at Angle of Attack: A Study of the Separation Point," Journal of Applied Mech, March 1972, pp. 7-12.

19. Briley, W. R., "A Numerical Study of Laminar Separation Bubbles Using the Navier-Stokes Equation", J. Fluid Mech. 47, Part 4, 1971, pp. 713-736.

20. Leal, L. G., "Steady Separated Flow in a Linearly-Decelerated Free Stream", Journal of Fluid Mechanics,59, 3, 1973, pp. 513-535.

21. Lee, C. H., "On Laminar Boundary Layer Separations", Thesis, State Univ. of N. Y. at Buffalo (Univ. Microfilms 72-27-260), 1972.

22. Oswatitsch, K., "Die Abosungsbedingung von Grenzschichen", In: Grenzschich-forschung/Boundary Layer Research", IUTAM Symposium, Freiburg/Br. 1957,

Springer Verlag 1958, p. 357-367.

23. Thwaites, B., "Approximate Calculation of the Laminar Boundary Layer", Aero. Quart. I, Nov. 1949, p. 245.

24. Ting, Lu, "Pressure Distribution on a Surface with Large Normal Injection", AIAA Journal 4, Sept. 1969, pp, 1573-79.

25. Lees, L. and T. C. Su, "Viscous-Inviscid Flow Interaction in Stratified Flow over a Barrier", AFOSR TR-73-2319, (Calif. Inst. of Technol. Report), Sept. 1972.

26. Jobe, C. E. and O. Burggraf, "The Numerical Solution of the Asymptotic Equations of Trailing Edge Flow", Journal of Fluid Mech. (to be published).

27. Catherall, D., and Mangler, K. W., "The Integration of the Two-Dimensional Laminar Boundary-Layer Equations Past the Point of Vanishing Skin Friction", Journal Fluid Mech. 26, Part 1, 1966, pp. 163-182.

28. Goldstein, S., "On Laminar Boundary Layer Flow Near a Position of Separation", Quart. Journal of Mech. and Appl. Mech 1, 1948, 43

29. J. Schetz, Private Communication.

30. Garvine, R. W., "Upstream Influence in Viscous Interaction Problems", Phys. of Fluids 11, July 1968, pp. 1413-23.

31. Shamroth, S. J. and H. McDonald, "A New Solution of the Turbulent Near-Wake Recompression Problem", Aeronaut. Quarterly, May 1972, pp. 121-130.

32. Lighthill, M. J., "On Boundary Layers and Upstream Influence, I. A. Comparison between Subsonic and Supersonic Flows", Proc. Royal Soc. A, 1953, pp. 344-357.

33. Gault, D. E., "Boundary Layer and Stalling Characteristics of the NACA 63-009 Airfoil Section", NACA TN-1894, 1949.

34. Stratford, B. S., "The Prediction of the Turbulent Boundary Layer," Journal of Fluid Mech. 5, 1959, pp, 1-16.

APPENDIX A

Approximate Expression for Displacement Thickness

A simplified version of Eq. (7b) can be derived by developing an analytical approximation to the integral term as follows. Noting that the radical in the integrand is simply u_{outer}, and that the equality of stream function requires $u_{outer}dy = u_B dy_B$, we obtain

$$\int_{y_j}^{\delta} \left(1 - \sqrt{\frac{u_B^2}{u_e^2} - \frac{C_p}{1-C_p}}\right) dy \approx \delta - y_j - \delta_B \int_{\eta_j}^{1} \frac{u_B}{u_e} d\eta \qquad (A-1)$$

$$= \delta - y_j - \delta_B \left[\int_0^1 \frac{u_B}{u_e} d\eta - \int_0^{\eta_j} \frac{u_B}{u_e} d\eta\right]$$

$$= \delta - y_j - \delta_B \left[\left(\frac{\delta_B - \delta_B^*}{\delta_B}\right) - \left(\frac{y_j}{\delta_B}\right)^2 \left(1 - \frac{\eta_j^2}{2} + \frac{\eta_j^3}{5}\right)\right]$$

$$(A-2)$$

where $\eta = y/\delta_B$, δ_B and δ_B^* pertain to the <u>local</u> basic inviscid flow u_e (not u_{e_0}), and the Karman-Pohlhausen polynomial approximation $u_B(\eta)/u_e \approx 2\eta - 2\eta^3 + \eta^4$ has been used to evaluate the integral. Then by neglecting η_j^2 and η_j^3 as small compared to unity, we obtain upon substitution of A-2 in Eq. (7b) the final result given by Eq. (7c).

In the aforementioned expressions for δ^*, the value of the conespanding boundary layer thickness δ can be estimated from the well-known Thwaites formula as

$$\delta = \frac{\delta}{\theta^*}\,\theta^* \approx \frac{315}{37}\sqrt{.45\,\frac{1}{u_{e_0}^6}\int_0^x u_e^5 dx}$$

$$\approx \sqrt{\frac{1}{x}\,\frac{u_e}{u_{e_0}}\int_0^x \left(u_e/y_{e_0}\right)^5 dx}\quad \delta_B \qquad (A-3)$$

APPENDIX B

Properties of the Displacement Thickness Integral

The induced pressure field is governed by the global effect of the displacement thickness as shown in Eq. 8. Assuming for the moment that the viscous interaction-induced pressure gradient effect on $\delta*$ is confined to some region $x_i \leq x \leq x_f$, the integral in this Eq. can be written as

$$\int_0^\infty \frac{(x-\xi)(\frac{d\delta*}{dx})}{(x-\xi)^2+\delta*^2} d\xi \cong \int_0^{x_i} \frac{(x-\xi)\frac{d\delta_B*}{dx}}{(x-\xi)^2+\delta*^2} d\xi + \int_{x_i}^{x_f} \frac{(x-\xi)\frac{d\delta*}{dx}}{(x-\xi)^2+\delta*^2} d\xi + \int_{x_f}^\infty \frac{(x-\xi)\frac{d\delta*}{dx}}{(x-\xi)^2+\delta*^2} d\xi \quad \text{(B-1)}$$

where $x_i (\rightarrow 0)$ and $x_f >> x_c$ are the effective start and end of the interaction region, respectively. Here, the first and third integrals account for the constant pressure regions of the basic flow while the second is the contribution of the interaction region. We now consider Eq. B-1 applied to some streamwise point x within the interval $x_i \leq x \leq x_f$ and proceed to examine each of the three integrals on the RHS.

Taking note of the fact that $\delta_B* \cong 1.73\varepsilon \ (x \sqrt{1-C_{p,basic}})^{-1/2}$ and choosing x_i small enough that $C_{p,basic} (x_i) \simeq 0$, the first integral can be rewritten as

$$\frac{2}{1.73\varepsilon} \int_0^{x_i} \frac{(x-\xi)(d\delta_B*/dx)d\xi}{(x-\xi)^2+\delta*^2(x)} \simeq \int_0^{x_i} \frac{(x-\xi)d\xi}{\sqrt{\xi}[(x-\xi)^2+\delta*^2(x)]} \quad \text{(B-2)}$$

Now since $\delta*\sim\varepsilon$ is small compared to unity and since Eq. B-1 pertains to $x \geq x_i$, $\delta*$ makes a significant contribution to the integrand only within a distance $\ell \approx \delta_B*(x_i)$ of the end point $\xi = x_i$; consequently, this RHS integral can be further decomposed into the two parts

$$\cong \int_0^{x_i - \ell} \frac{d\xi}{\sqrt{\xi}\,(x-\xi)} + \frac{1}{\sqrt{x_i}} \int_{x_i - \ell}^{x_i} \frac{(x-\xi)\,d\xi}{(x-\xi)^2 + \ell^2}$$

which standard integral tables evaluate as

$$= \frac{1}{\sqrt{x}} \log\left[\frac{x + (x_i - \ell) + 2\sqrt{x(x_i - \ell)}}{x - (x_i - \ell)}\right] + \frac{1}{2\sqrt{x_i}} \log\left[\frac{(x-x_i)^2 + \ell^2}{(x-x_i)^2 + \ell^2 + 2\ell(x-x_i)}\right] \qquad \text{(B-3)}$$

We note that the second term vanishes while the first gives a non-singular result at $x \to x_i$. Most importantly, we note that choosing $x_i = \ell = \delta_B^*(x_i)$ eliminates the first term at <u>all</u> $x \geq x_i$, leaving only the second term which vanishes at $x = x_i$ <u>and</u> as $x \gg x_i$. The first integral in B-1 can therefore be made negligiable by this suitably small choice of x_i.[†]

Substituting the value of δ_B^* into the third integral on the RHS of (B-1) and proceeding in the same manner as we did with (B-2), this integral can be written

$$\frac{2}{1.73\epsilon} \int_0^\infty \frac{(x-\xi)\dfrac{d\delta_B^*}{dx}\,d\xi}{(x-\xi)^2 + \delta^{*2}} \int_{x_f + k}^\infty \frac{d\xi}{\sqrt{\xi}\,(x-\xi)} + \frac{1}{\sqrt{x_f}} \int_{x_f}^{x_f + k} \frac{(x-\xi)d\xi}{(x-\xi)^2 + k^2} \qquad \text{(B-4)}$$

where the δ^{*2} term in the integrand is presumed to have a negligiable effect beyond some small distance k from x_f. Again using standard integral tables, the RHS becomes

$$= \frac{1}{\sqrt{x}} \log\left[\frac{x_f + k - x}{x_f + k + x - 2\sqrt{x(x_f + k)}}\right] + \frac{1}{2\sqrt{x_f}} \log\left[\frac{(x_f + k - x)^2 + k^2}{(x_f - x)^2 + k^2}\right]$$

[†]This choice of x_i is analogous to the use of a Lighthill correction factor in Eq. 8c to wipe out the leading edge contribution in the alternative singular airfoil integral formulation.

which we see vanishes at $x = x_f$ and as $x \ll x_f$ for all k provided x_f is taken sufficiently large.

We have thus shown that provided x_i and x_f are chosen sufficiently small and large, respectively, only the second integral on the RHS of Eq. B-1 does in fact effectively contribute to the induced pressure field as assumed, and that ΔC_p vanishes at these end points. Moreover, since this type of integral is in effect a solution to LaPlaces Equation, $d\Delta C_p/dx$ inherently vanishes at these points as well.[26] In carrying out numerical evaluations of the second integral, it proves convenient to elimmate the derivative of $\delta*$ through integration by parts so as to obtain

$$\int_{x_i}^{x_f} \frac{(x-\xi)\frac{d\delta*}{dx}}{(x-\xi)^2 + \delta*^2}\, d\xi = \left[\frac{(x-\xi)\,*}{(x-\xi)^2 + \,*^2_{(x)}} \right]_{x_i}^{x_f} - \int_{x_i}^{x_f} \frac{[(x-\xi)^2 - \delta*^2]\delta*}{(x-\xi)^2 + \delta*^2}\, d\xi \qquad (B-5)$$

DISTURBED INVISCID FLOW

EDGE OF BOUNDARY LAYER $\delta(x)$

ROTATIONAL INVISCID FLOW

$y = y_j(x)$

EQUILIBRIUM VISCOUS SUBLAYER

BODY

y

x_0

x

p

TYPICAL UNINTERACTED PRESSURE DISTRIBUTION

$x = 0$

x_0

x_c

Fig. 1: Schematic of Three Layered Flow Model

32
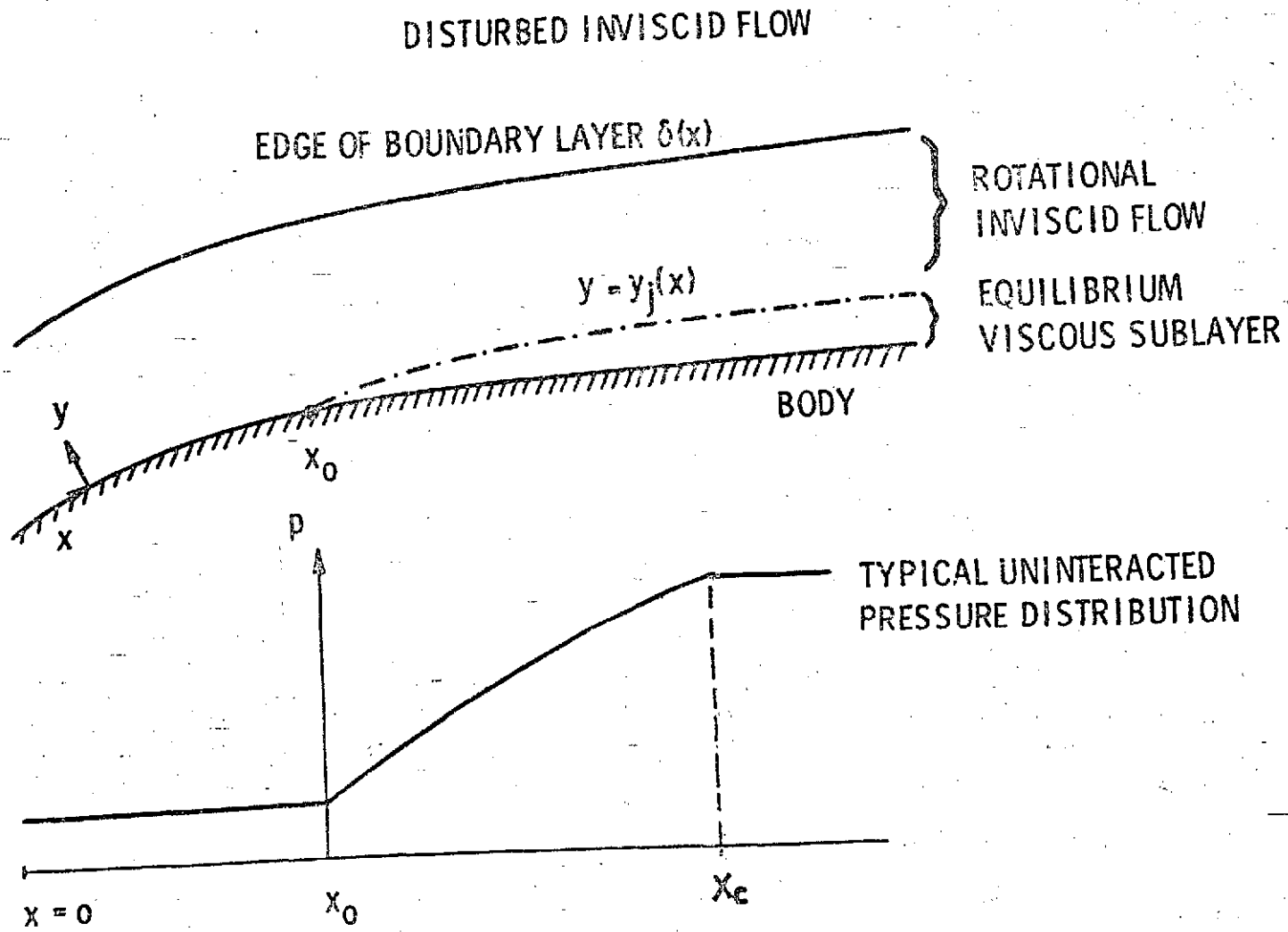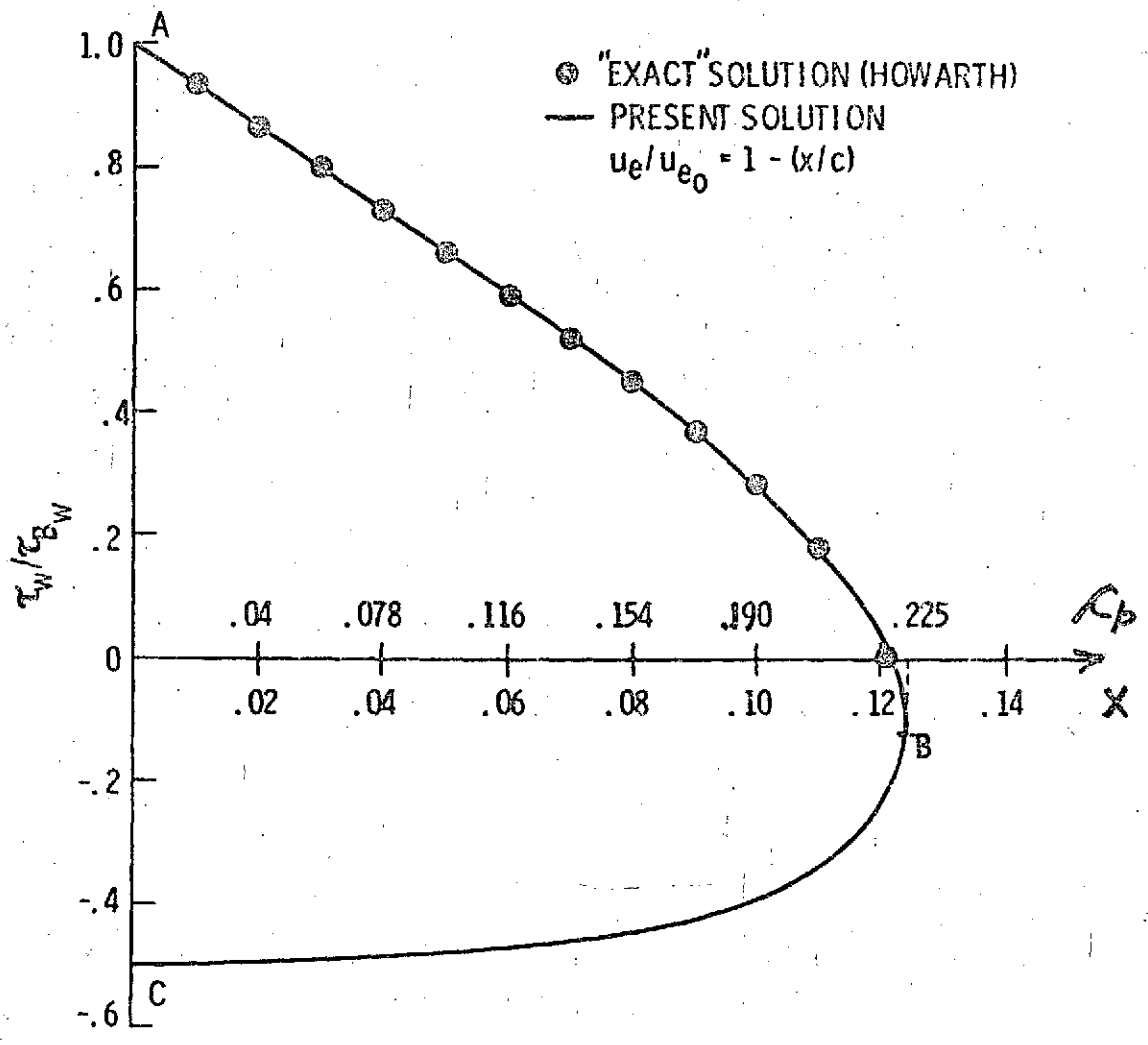
Fig. 2: Double-Valued Nature of Skin-Friction for a Linearly Retarded Basic Inviscid Flow

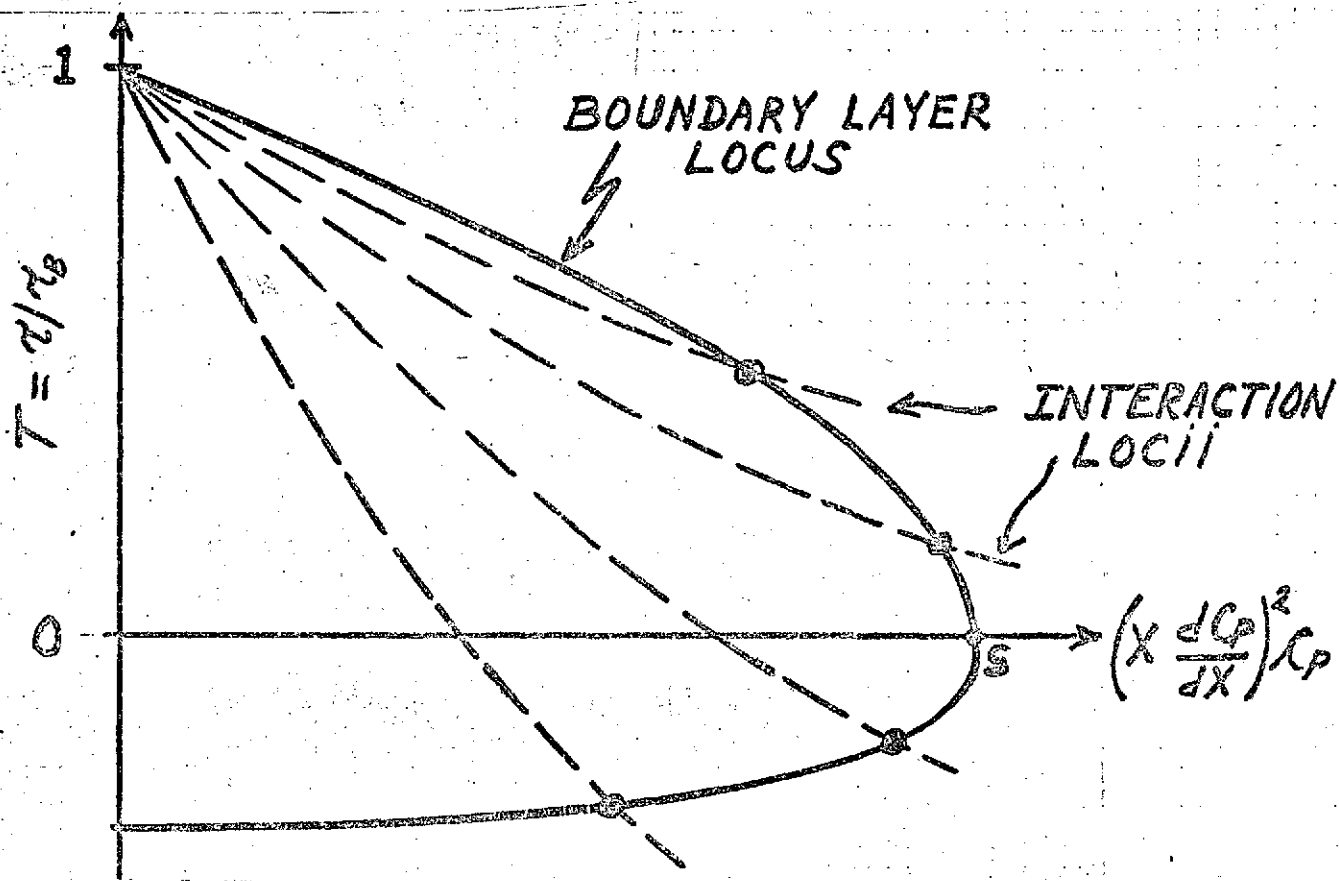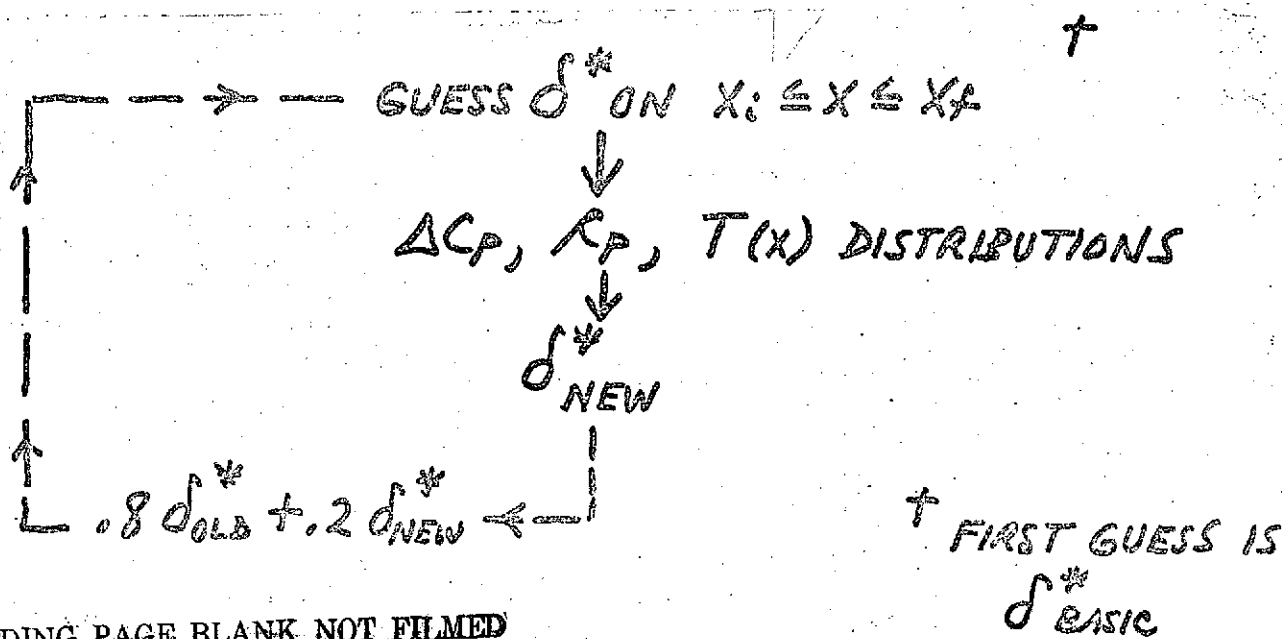Fig. 3. Schematic of Interactive Solution.
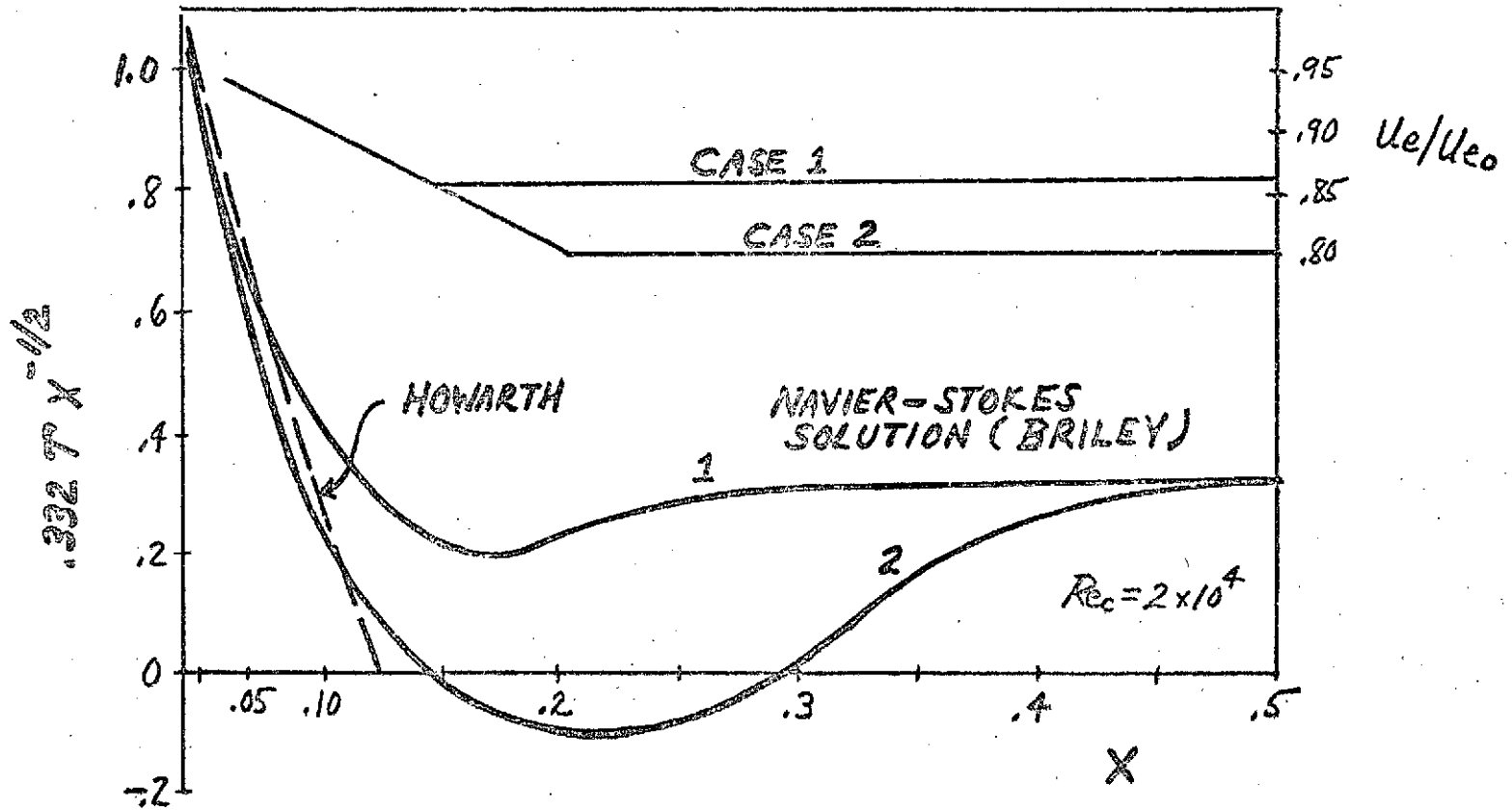
Fig. 4. Global Iteration Procedure.

34

Fig. 5: Interacted Shear-Stress Distribution for Linearly
Retarded Flow with and without Separation
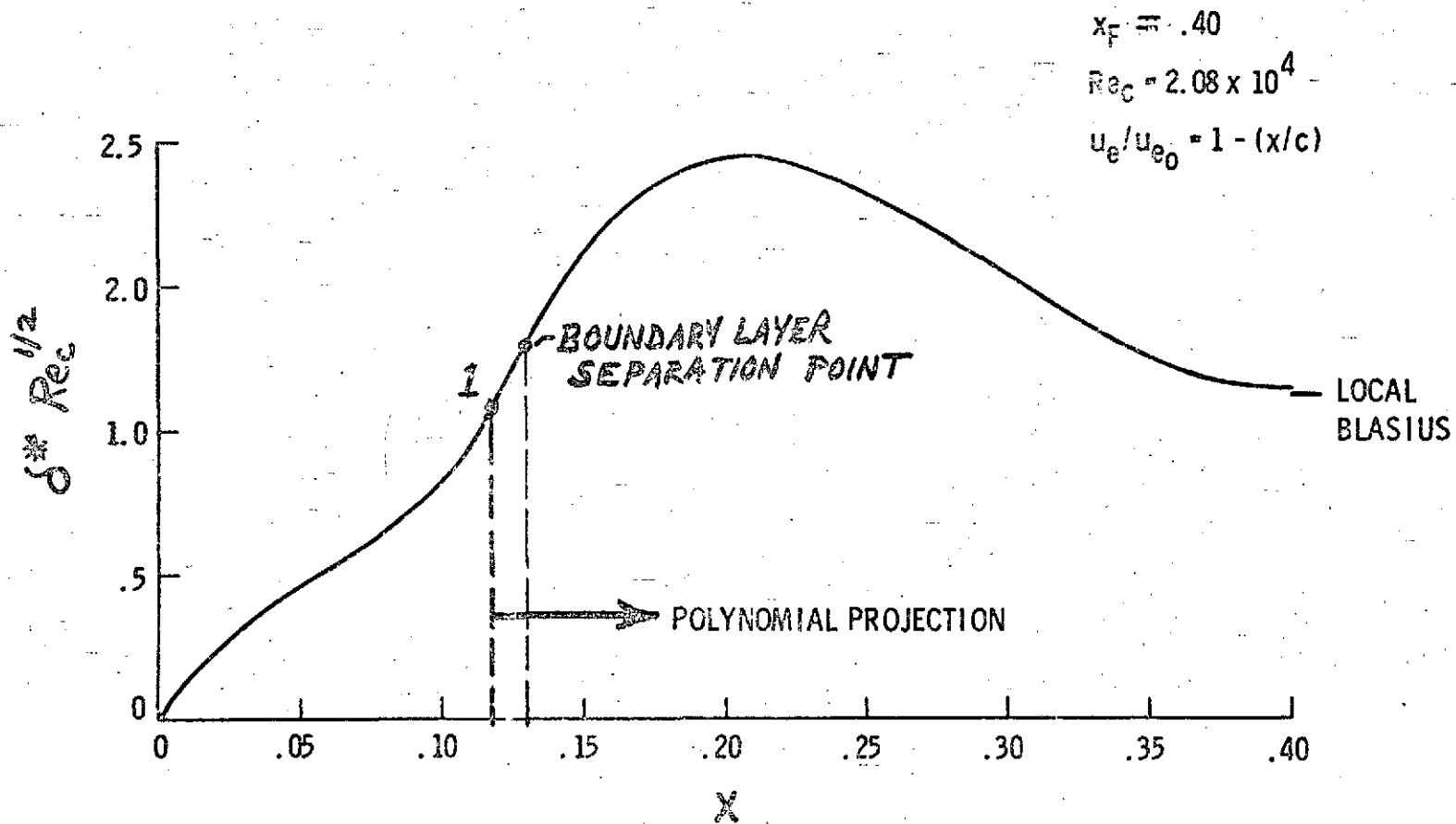
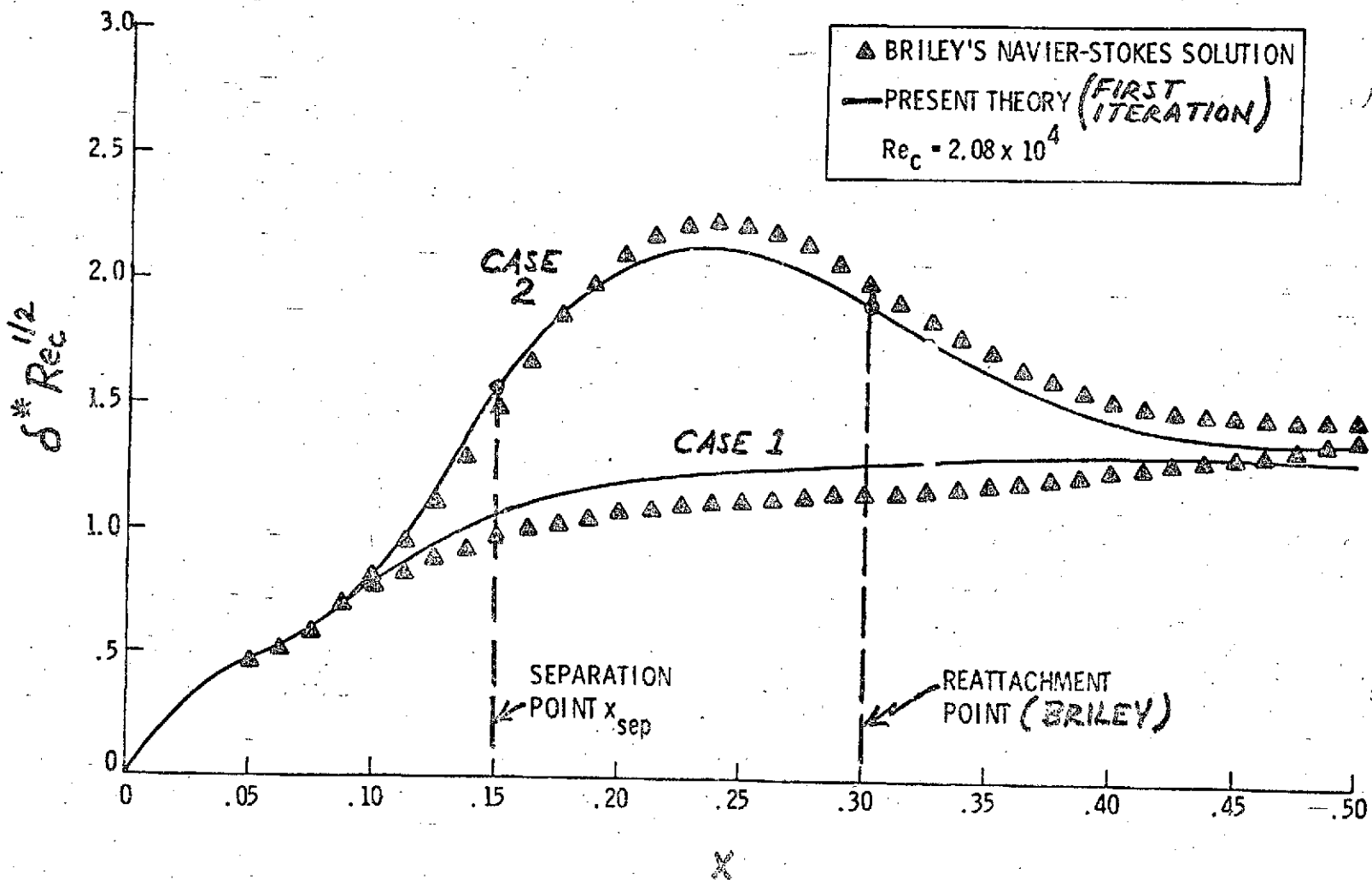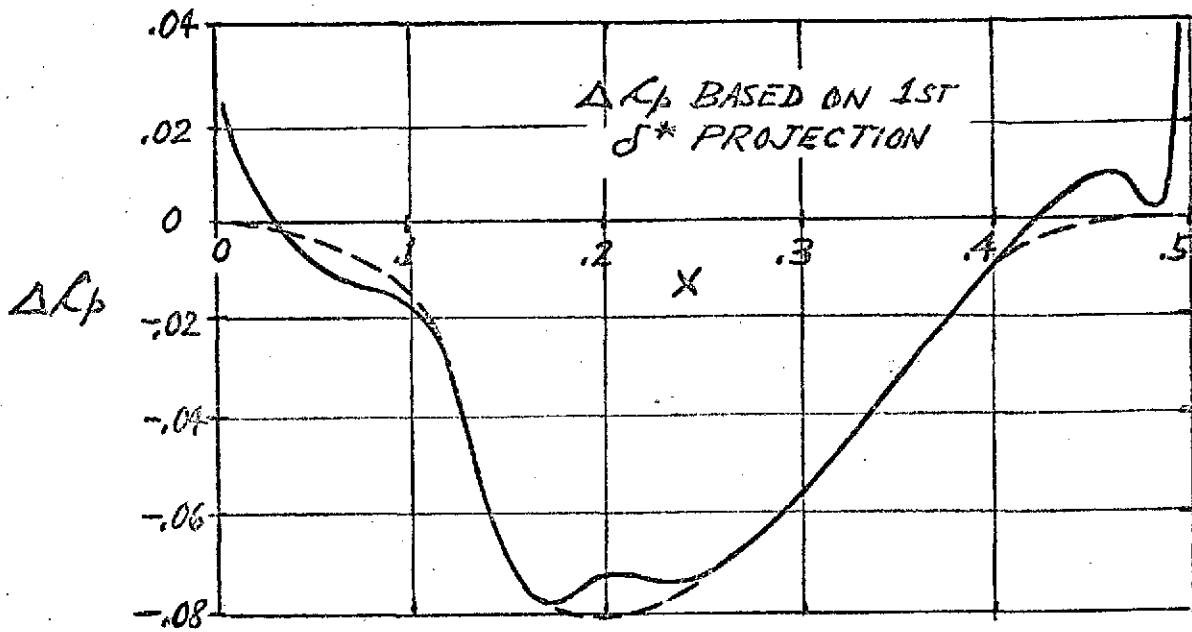Fig.6: First Projection of Displacement Thickness Through
Separation Region
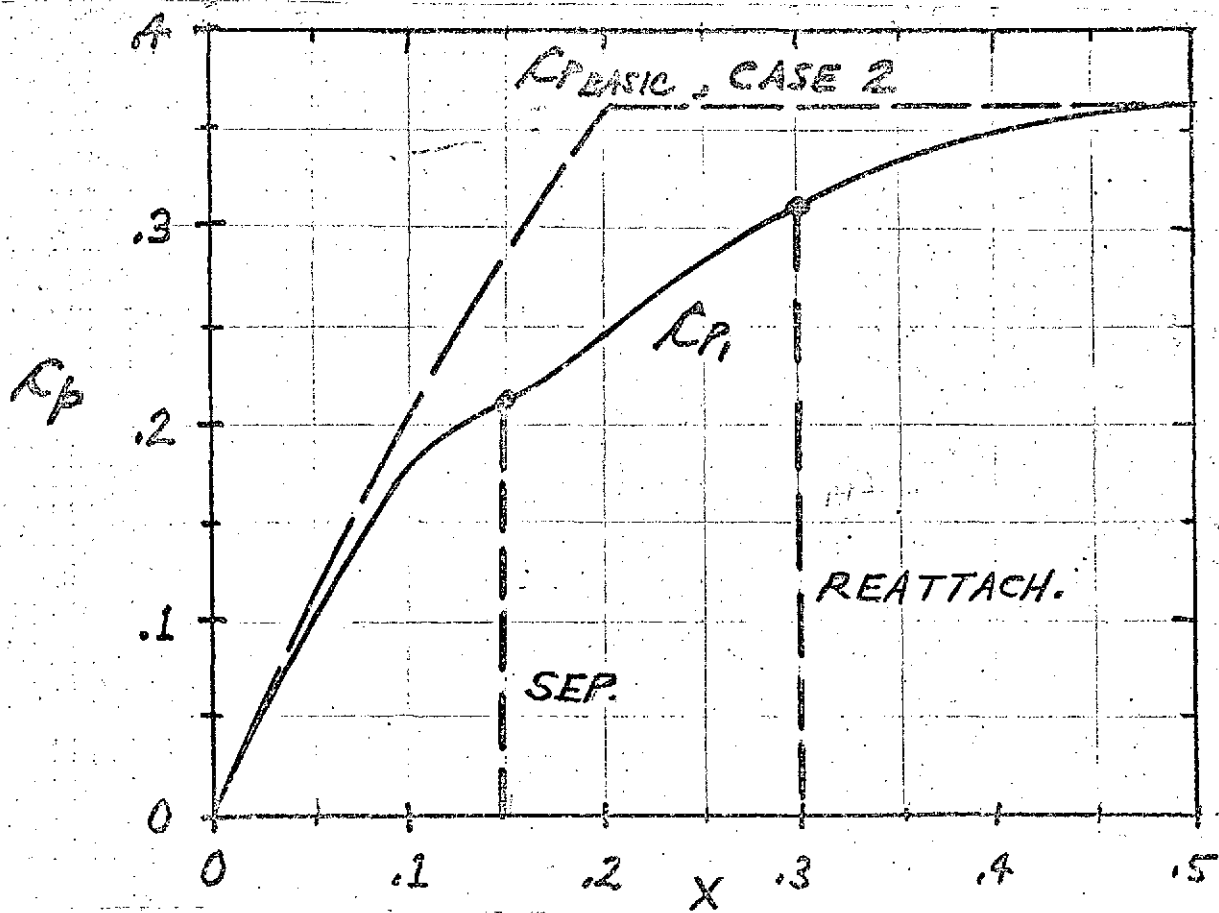
Fig. 7: Interacted Displacement Thickness Solution for
Separated and Unseparated Linearly Retarded Flow

Fig. 8 Viscous-Inviscid Interaction Effect
on Pressure Distribution.